CENTER FOR TOKAMAK TRANSIENTS SIMULATION

CTTS Overview

Stephen C. Jardin

Theory and Simulation of Disruptions Workshop

PPPL, August 5-7, 2019

CTTS Participants

PHYSICS TEAM

- **PPPL**: C. Clauser, N. Ferraro, I. Krebs, S. Jardin, C. Liu, C. Zhao
- **GA**: V. Izzo, C. Kim ,L. Lao, B. Lyons, J. McClenaghan, P. Parks
- **U. Wisc**: K. Bunkers, C. Sovinec, G. Wang, P. Zhu
- **Utah State U**: E. Held
- **Tech X:** E. Howell, J. King, S. Kruger
- **SBU:** R. Samulyak
- **HRS Fusion**: H. Strauss

HPC TEAM

- **RPI**: M. Shephard, S. Seol, W. Tobin
- **LBL:** N. Ding, X. Li, Y. Liu, S. Williams
- **PPPL**: J. Chen
- **SBU**: R. Samulyak

30 participants (part time)
9 institutions

Center for Tokamak Transient Simulations Outline

1. Code Descriptions

2. Forces due to Vertical Displacement Events

3. Disruption Mitigation via Impurity Injections
   3.1 Stand Alone
   3.2 via code coupling

4. Runaway Electrons interacting with MHD

5. High-Performance Computing

Center for Tokamak Transient Simulations Outline

1. Code Descriptions

2. Forces due to Vertical Displacement Events

3. Disruption Mitigation via Impurity Injections
   3.1 Stand Alone
   3.2 via code coupling

4. Runaway Electrons interacting with MHD

5. High-Performance Computing

M3D-C[1] and NIMROD solve 3D MHD Equations in Toroidal Geometry including Impurity Radiation and Runaway Electrons

$$\partial n_i/\partial t + \nabla \bullet (n_i \mathbf{V}) = \nabla \bullet D \nabla n_i + S_n$$

$$\partial n_Z^{(j)}/\partial t + \nabla \bullet (n_Z^{(j)} \mathbf{V}) = \nabla \bullet D \nabla n_Z^{(j)} + I_Z^{(j-1)} n_Z^{(j-1)} - \left(I_Z^{(j)} + R_Z^{(j)} \right) n_Z^{(j)} + R_Z^{(j+1)} n_Z^{(j+1)} + S_Z^{(j)}$$

$$\left.\begin{aligned} \partial \mathbf{A}/\partial t &= -\mathbf{E} - \nabla \Phi \\ \nabla_\perp \bullet \frac{1}{R^2} \nabla \Phi &= -\nabla_\perp \bullet \frac{1}{R^2} \mathbf{E} \\ \mathbf{B} &= \nabla \times \mathbf{A} \end{aligned}\right\} \text{M3D-C1} \qquad \left.\begin{aligned} \partial \mathbf{B}/\partial t &= -\nabla \times \mathbf{E} \\ \nabla \bullet \mathbf{B} &= 0 \end{aligned}\right\} \text{NIMROD}$$

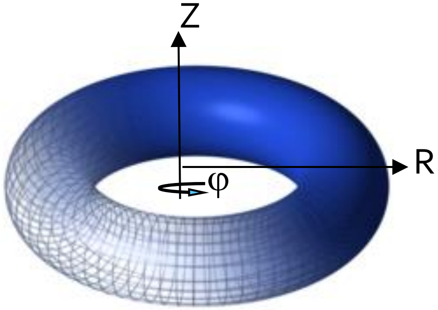

$$\rho(\partial \mathbf{V}/\partial t + \mathbf{V} \bullet \nabla \mathbf{V}) + \nabla p = \mathbf{J} \times \mathbf{B} - \nabla \bullet \mathbf{\Pi} - \varpi \mathbf{V} + \mathbf{S}_m, \qquad \mathbf{E} + \mathbf{V} \times \mathbf{B} = \eta(\mathbf{J} - \mathbf{J}_{RA}) + \mathbf{S}_{CD}$$

$$\frac{3}{2}\left[\frac{\partial p_e}{\partial t} + \nabla \bullet \left(p_e \mathbf{V} \right) \right] = -p_e \nabla \bullet \mathbf{V} + \mathbf{J} \bullet \mathbf{E} - \nabla \bullet \mathbf{q}_e + Q_\Delta + S_{eE} \qquad \mathbf{q}_{e,i} = -\kappa_{e,i} \nabla T_{e,i} - \kappa_{\parallel e,i} \nabla_\parallel T_{e,i}$$

$$\frac{3}{2}\left[\frac{\partial p_i}{\partial t} + \nabla \bullet \left(p_i \mathbf{V} \right) \right] = -p_i \nabla \bullet \mathbf{V} - \mathbf{\Pi}_i : \nabla \mathbf{V} - \nabla \bullet \mathbf{q}_i - Q_\Delta + \tfrac{1}{2} \varpi V^2 + S_{iE}$$

- Also, separate equations for resistive wall and vacuum regions
- Different options for Runaway Electron current $\mathbf{J}_{RA}$
- Option for energetic ion species (not used here)

M3D-C^1 and NIMROD have very different numerical implementations

	M3D-C^1	**NIMROD**
Poloidal Direction	Tri. C^1 Reduced Quintic FE	High. Order quad C^0 FE
Toroidal Direction	Hermite Cubic C^1 FE	Spectral
Magnetic Field	$\mathbf{B} = \nabla\psi\times\nabla\varphi - \nabla_\perp f' + F\nabla\varphi$	$\mathbf{B} = B_r\widehat{R} + B_z\hat{Z} + B_\varphi\widehat{\varphi}$
Velocity Field	$\mathbf{V} = R^2\nabla U\times\nabla\varphi + \omega R^2\nabla\varphi + R^{-2}\nabla_\perp\chi$	$\mathbf{V} = V_r\widehat{R} + V_z\hat{Z} + V_\varphi\widehat{\varphi}$
Coupling to Conductors	same matrix	Separate matrices w interface

Both codes use:

- Split Implicit Time advance
- Block-Jacobi preconditioner based on SuperLU_DIST
- GMRES based iterative solvers
- Impurity ionization and recombination rates from KPRAD

Center for Tokamak Transient Simulations Outline

1. Code Descriptions

2. Forces due to Vertical Displacement Events

3. Disruption Mitigation via Impurity Injections
   3.1 Stand Alone
   3.2 via code coupling

4. Runaway Electrons interacting with MHD

5. High-Performance Computing

Vertical Displacement Events: (VDEs)

K. Bunkers: The influence of boundary conditions on NIMROD Axisymmetric VDE computations

C. Sovinec: Update on axisymmetric VDE benchmarking

Strauss: Thermal quench and asymmetric wall force in ITER disruptions

Clauser: Vertical Force during VDEs in ITER and the role of halo currents

Jardin: Coupling of M3D-C^1 to Carridi

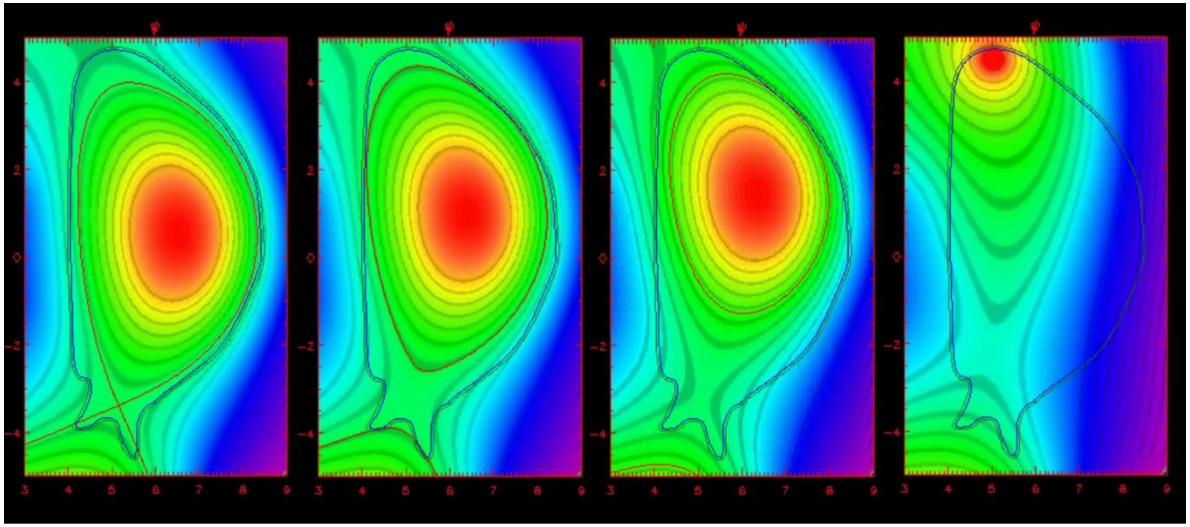

Equilibrium Wall contact Start TQ Final

5.3 T 15MA ITER

M3D-C¹ is being interfaced with the CARRIDI engineering code to produce realistic forces for ITER

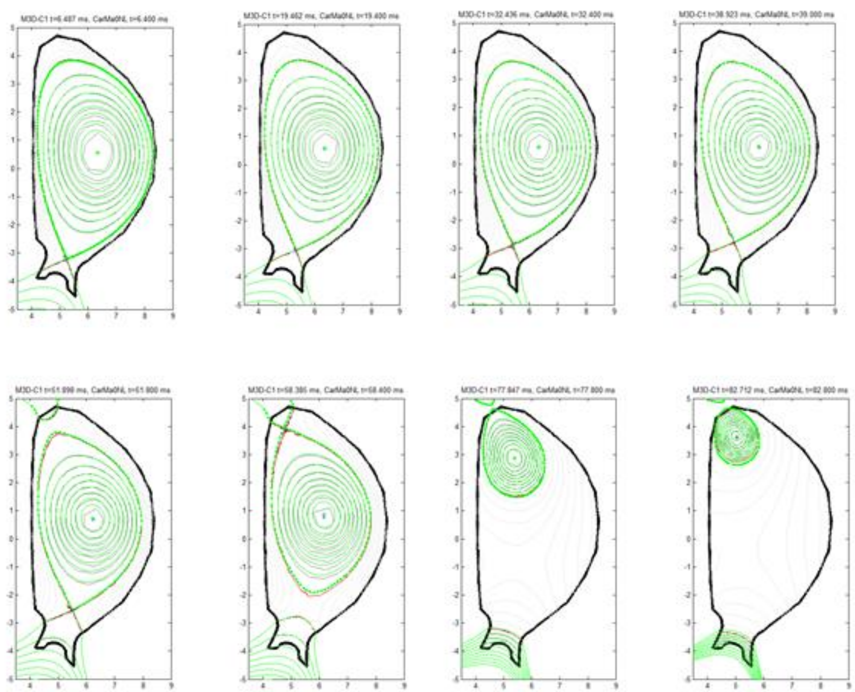

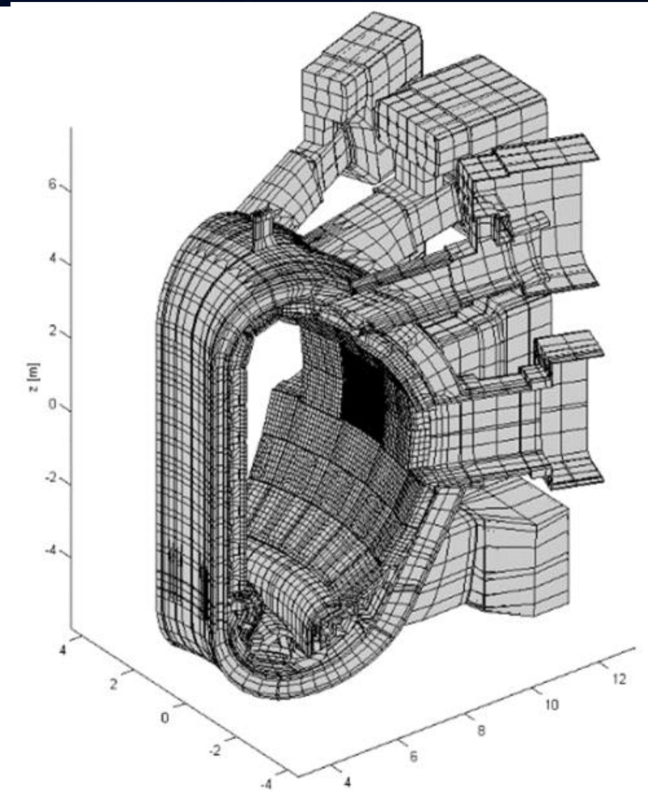

- CARRIDI is presently interfaced with the 2D equilibrium evolution code CARMA0NL
- Above benchmark between M3D-C¹ & CARMA0NL was presented at 2019 EPS

- CARRIDI detailed electro-magnetic model of ITER structure.
- Now interfacing M3D-C¹ VDE simulation with CARRIDI to extend analysis to 3D plasma

C. Clauser, F. Villone

Center for Tokamak Transient Simulations
Outline

1. Code Descriptions

2. Forces due to Vertical Displacement Events

3. Disruption Mitigation via Impurity Injections
   3.1 Stand Alone
   3.2 via code coupling

4. Runaway Electrons interacting with MHD

5. High-Performance Computing

Disruption Mitigation via Impurity Injections -- Stand Alone

B. Lyons … Recent progress in 3D modeling of disruption mitigation

V. Izzo … Modeling of shell pellet injection for disruption mitigation on DIII-D

S. Jardin … Modeling of Electromagnetic pellet injector in NSTX-U

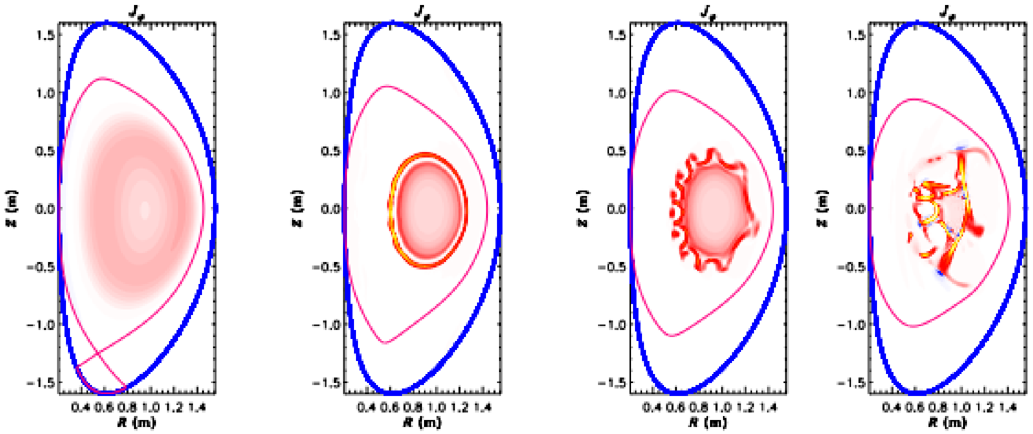

Ferraro, NF, 2019

Electromagnetic pellet injector offers advantages for ITER; proposal to test on NSTX-U

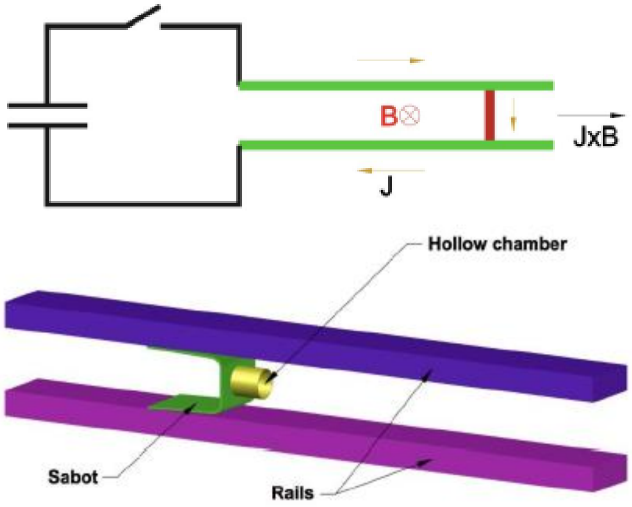

- Very fast response time (2-3 ms)
- Speeds up to 1 km/s
- High resolution modeling of 1 mm Carbon pellet as 2.5 cm (poloidal) x 25 cm (toroidal) Gaussian source

Electron Temperature

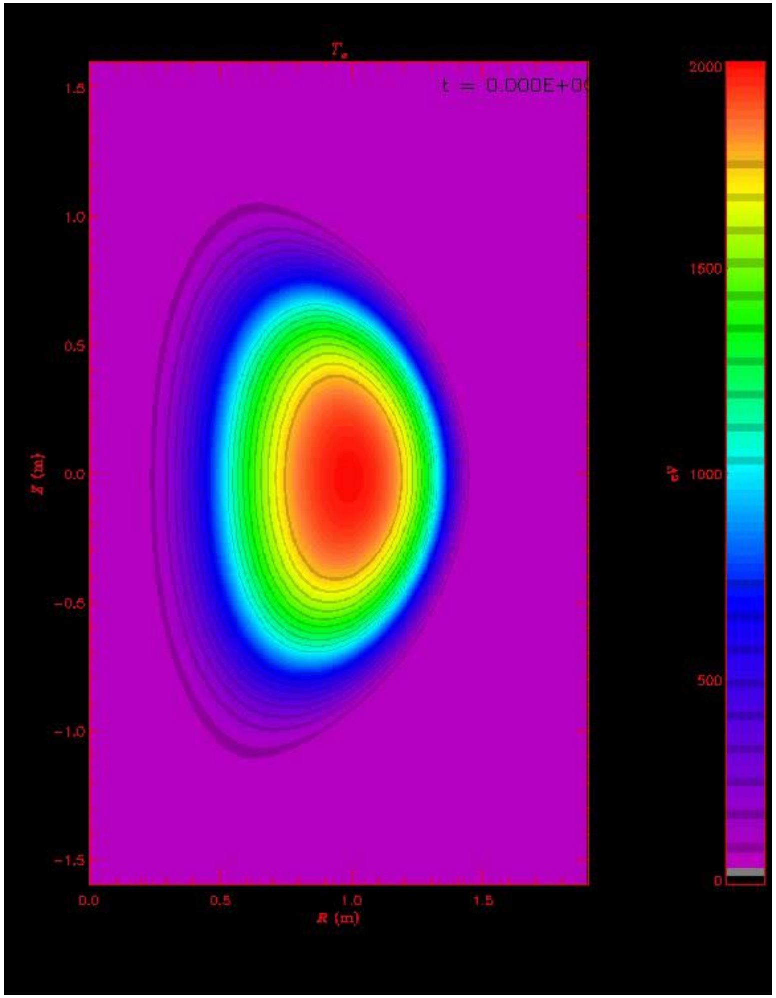

Te(0) = 2 keV

n(0) = 2 x 10^{19} m

I_P = 600 kA

βp = 0.73

li(3) = 0.6

R. Raman

4 time slices in a M3D-C¹ simulation of a 1 mm Carbon pellet injected into NSTX-U via EPI

Injection Plane Contours at different times

Change in Electron Temp.

(a) - 0.6 keV
(b) - 1.7 keV
(c) - 1.7 keV
(d) -1.7 keV

Carbon Density:

(a) 6.8 10^{19} m^{-3}
(b) 5.2 10^{19} m^{-3}
(c) 5.2 10^{19} m^{-3}
(d) 3.1 10^{19} m^{-3}

Radiation source:

(a) - 3.2. GW/m^3
(b) - 1.0 GW/m^3
(c) - 1.1 GW/m^3
(d) - 0.4 GW/m^3

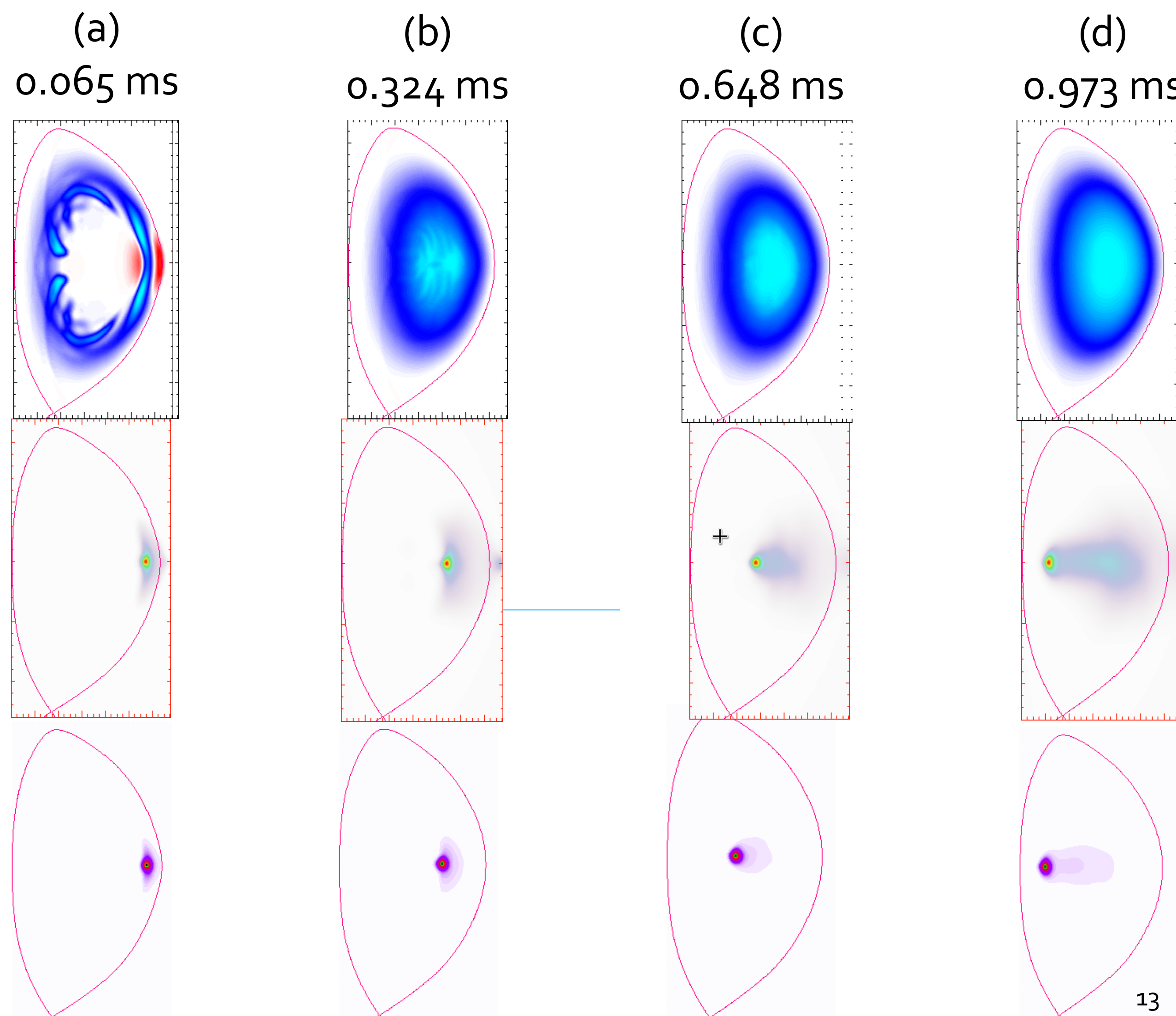

Contours at t=0.13 ms at 4 toroidal locations for M3D-C¹ simulation of 1 mm Carbon EPI in NSTX-U

Same time (t=0.130 ms), different toroidal locations

(a) $\varphi = 0^o$ (b) $\varphi = 90^o$ (c) $\varphi = 180^o$ (d) $\varphi = 270^o$

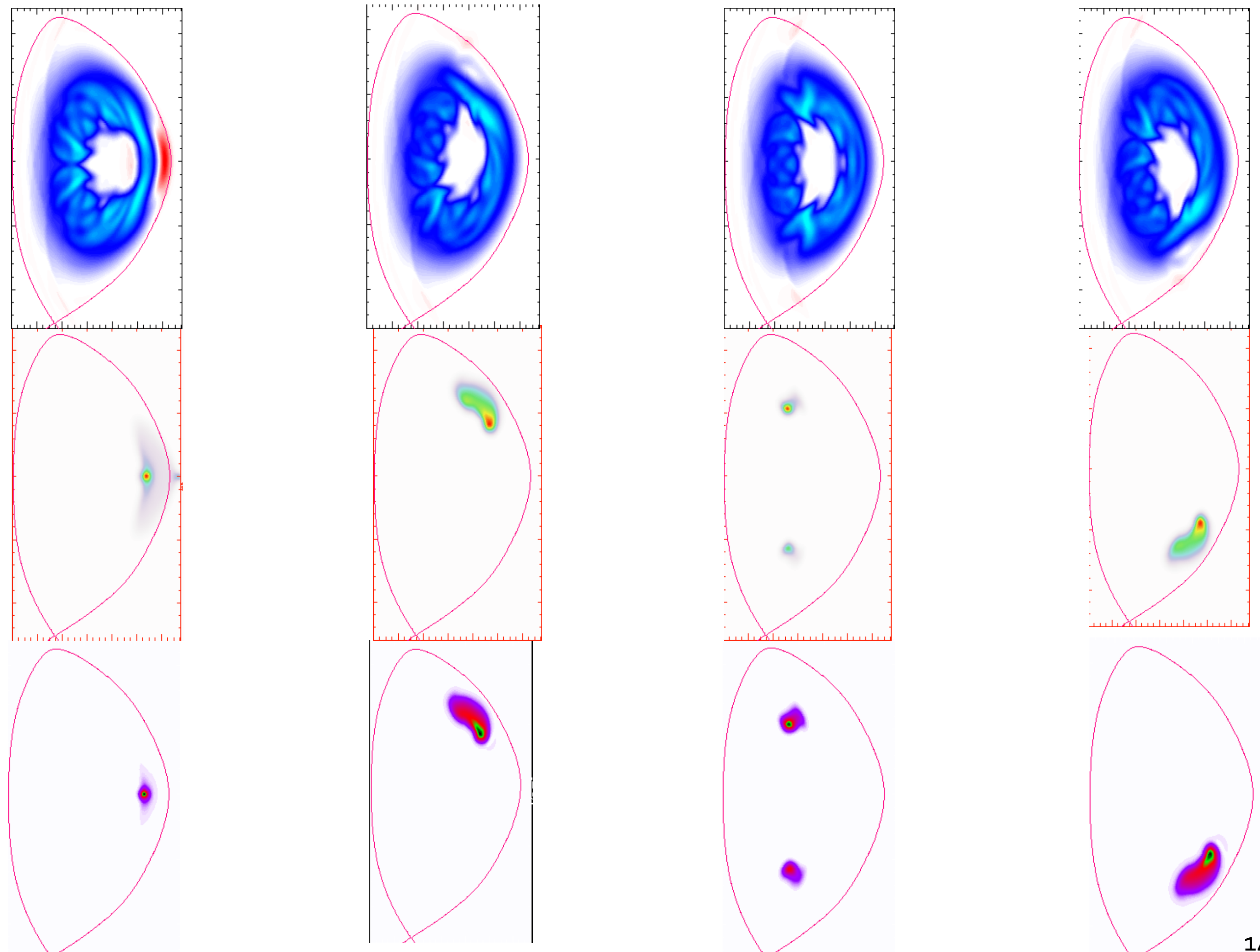

Change in Electron Temp.

(a) – 969. eV
(b) - 1062 eV
(c) – 1034 eV
(d) - 1067eV

Carbon Density:

(a) 8.20 10^{19} m^{-3}
(b) 1.86 10^{19} m^{-3}
(c) 0.07 10^{19} m^{-3}
(d) 1.86 10^{19} m^{-3}

Radiation source:

(a) - 4400 MW/m^3
(b) - 40. MW/m^3
(c) - 0.5 MW/m^3
(d) -40. MW/m^3

Convergence study of toroidal resolution and toroidal pellet extent

Plasma properties and pellet source distributed over the Gaussian Distribution:

$$S = \frac{1}{(2\pi)^{3/2} V_p^2 V_t} \exp\left[-\frac{(R-R_p)^2 + (Z-Z_p)^2}{2V_p^2} - \frac{RR_p\left(1-\cos(\varphi-\varphi_p)\right)}{V_t^2} \right]$$

nplane	V_t
8	1.00
16	0.50
32	0.25

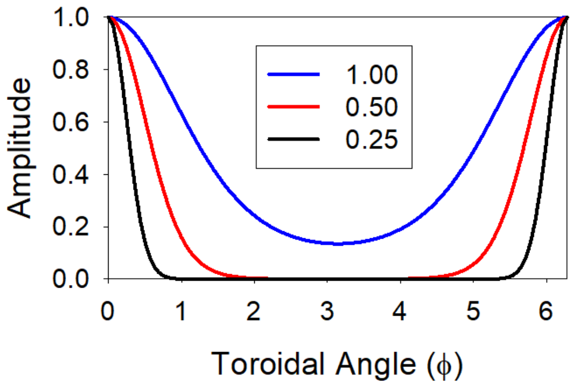

Convergence study in # of toroidal planes indicates the highest toroidal resolution used so far may not be high enough.....Still in progress.

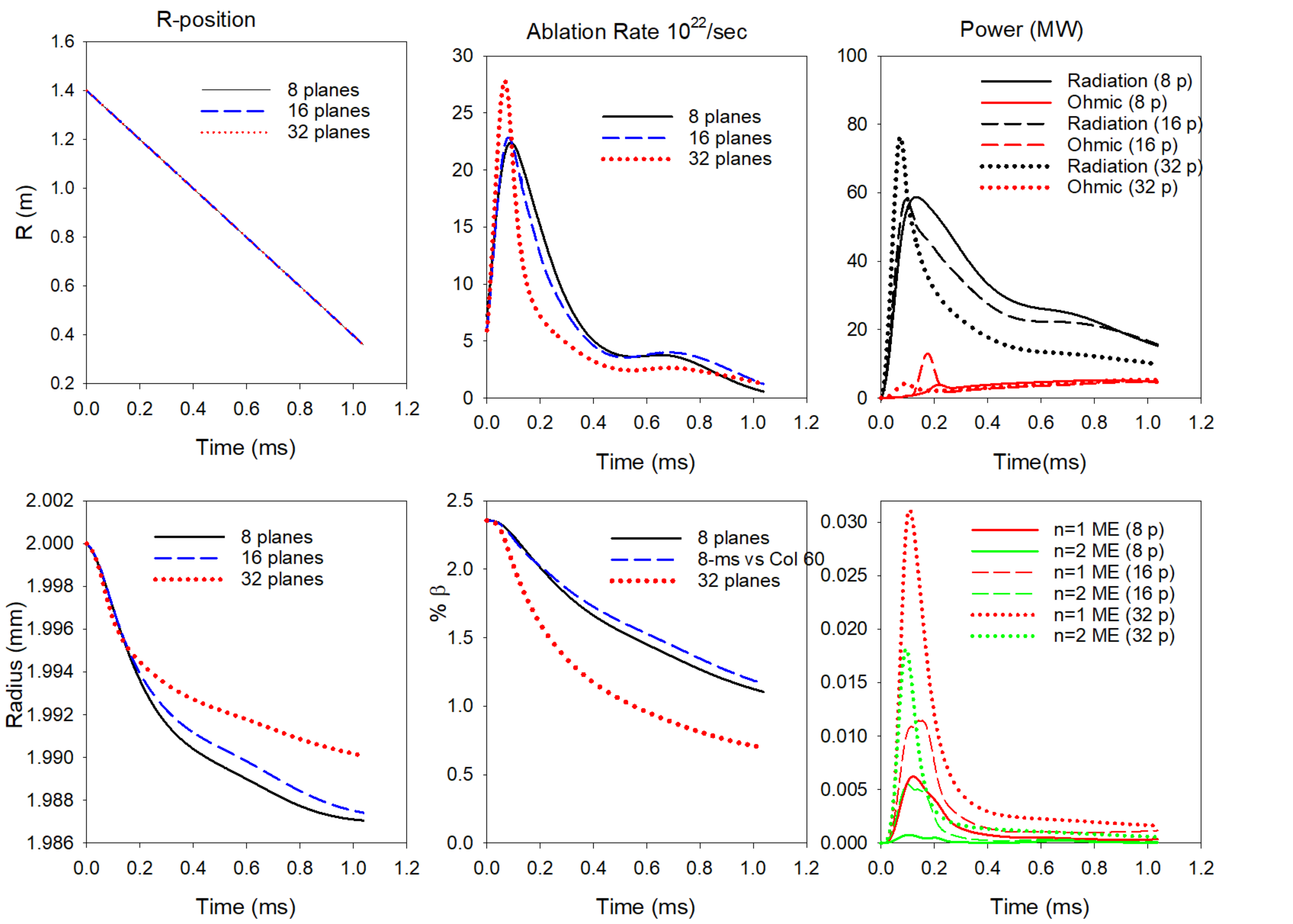
R-position
R (m)
Time (ms)
8 planes
16 planes
32 planes
Ablation Rate 10^{22}/sec
Time (ms)
8 planes
16 planes
32 planes
Power (MW)
Time(ms)
Radiation (8 p)
Ohmic (8 p)
Radiation (16 p)
Ohmic (16 p)
Radiation (32 p)
Ohmic (32 p)
Radius (mm)
Time (ms)
8 planes
16 planes
32 planes
% β
Time (ms)
8 planes
8-ms vs Col 60
32 planes
Time (ms)
n=1 ME (8 p)
n=2 ME (8 p)
n=1 ME (16 p)
n=2 ME (16 p)
n=1 ME (32 p)
n=2 ME (32 p)

Te contours for different toroidal resolutions (injection plane)

t = 0.065ms, T_{max} = 2000ev

t = 0.130ms, T_{max} = 1500ev

t = 0.650ms, T_{max} = 0270ev

t = 0.1000ms, T_{max} = 0270ev

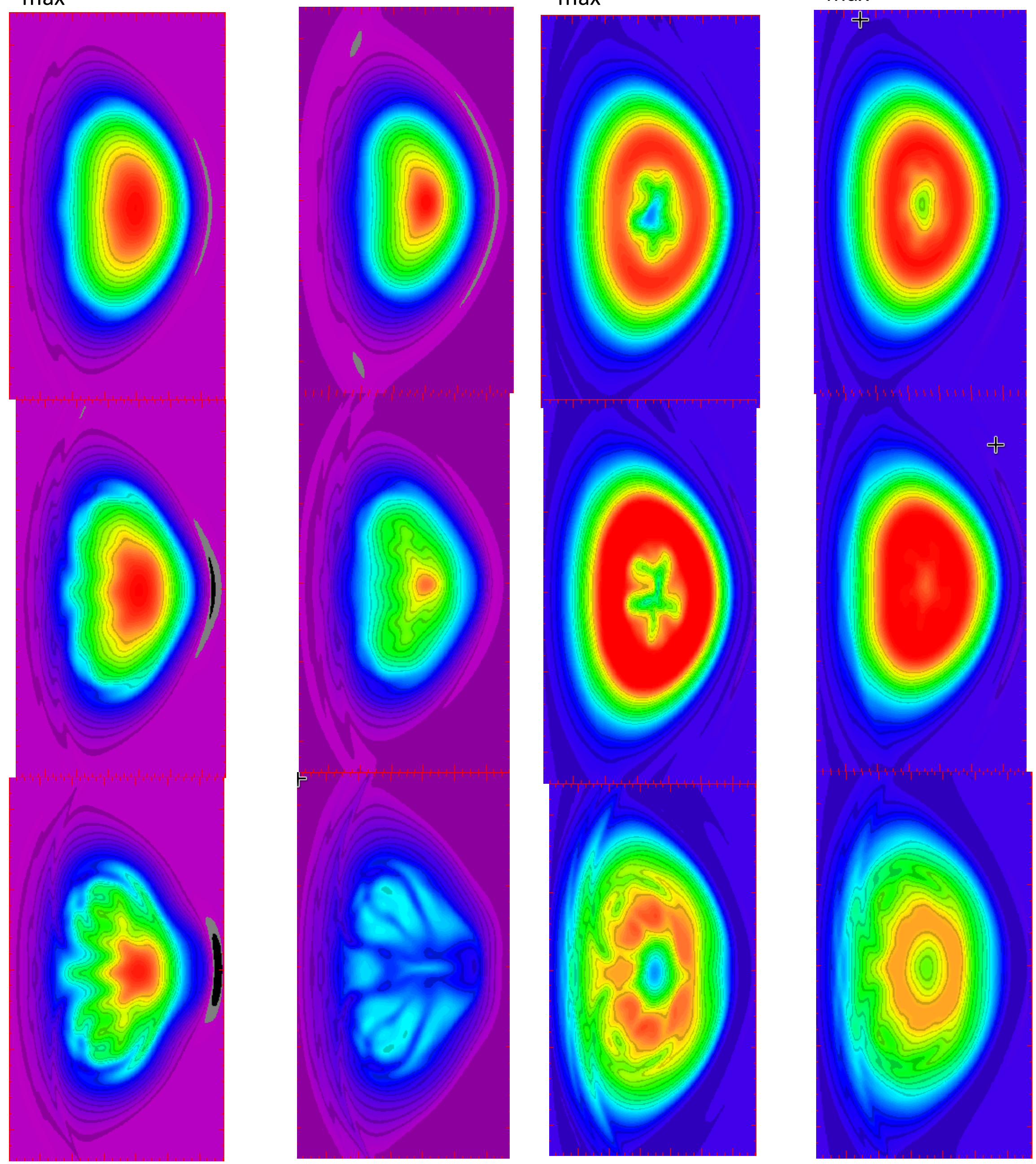

8 planes
var_tor = 1.00 m

16 planes
var_tor = 0.50 m

32 planes
var_tor = 0.25 m

Center for Tokamak Transient Simulations Outline

1. Code Descriptions

2. Forces due to Vertical Displacement Events

3. Disruption Mitigation via Impurity Injections
   3.1 Stand Alone
   3.2 via code coupling

4. Runaway Electrons interacting with MHD

5. High-Performance Computing

Disruption Mitigation via Impurity Injections – via code coupling

R. Samulyak…Simulation studies of the ablation of Neon pellets and SPI fragments for plasma disruption mitigation in tokamaks

NIMROD simulation domain showing ablated material obtained from LP code

LP simulation of pellet ablation cloud

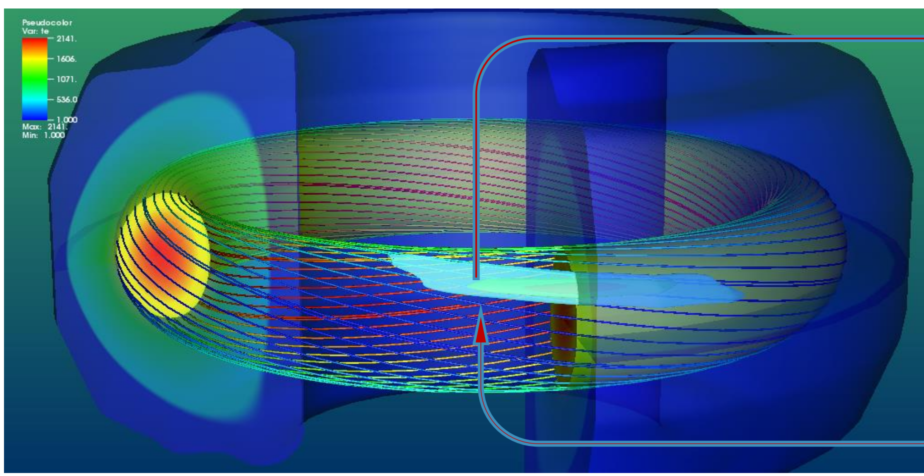

B, n_e, T_e from TK to LP

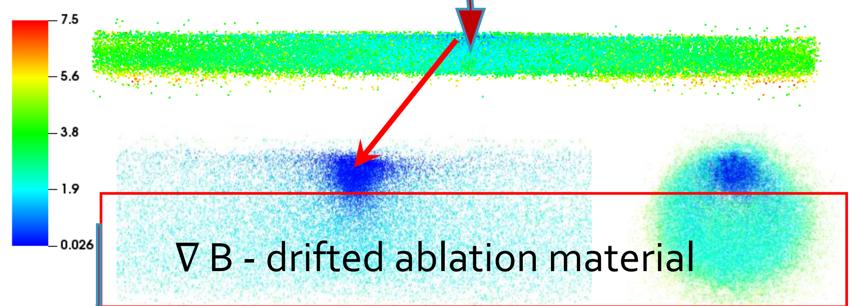

Mass flow, thermodynamic data, and energy sinks from LP to TK

Center for Tokamak Transient Simulations
Outline

1. Code Descriptions

2. Forces due to Vertical Displacement Events

3. Disruption Mitigation via Impurity Injections
   3.1 Stand Alone
   3.2 via code coupling

4. Runaway Electrons interacting with MHD

5. High-Performance Computing

Runaway Electrons interacting with MHD

C. Zhao .. Simulation of MHD instabilities with runaway electron current using M3D-C1

G. Wang ...Reduced models of runaway electrons in NIMROD ... (poster)

- A collaboration between PPPL, GA, and ORNL is initialized to couple both M3D-C1 and NIMROD with KORC to model runaway electron diffusion and its back reaction to MHD instabilities

KORC: Highly scalable PIC RE code using GPUs (ORNL)

Perturbed current of (1,1) mode From M3D-C1 without RE current

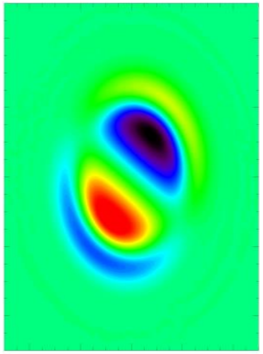

Perturbed current of (1,1) mode with RE current

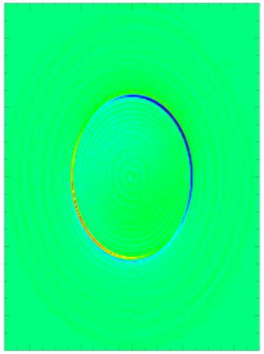

C. Liu, C. Zhao

Center for Tokamak Transient Simulations
Outline

1. Code Descriptions

2. Forces due to Vertical Displacement Events

3. Disruption Mitigation via Impurity Injections
   3.1 Stand Alone
   3.2 via code coupling

4. Runaway Electrons interacting with MHD

5. High-Performance Computing

Must Address Communication to Improve Scaling Performance

- SuperLU Preconditioners are essential for the solvers in M3D-C[1] and NIMROD
- Solver performance is dominated by MPI communications in the triangular solve
- Performance improvements in SpTRSV improves application performance and scalability

- COMPARED SIX MATRICES
  - 1 from FES code M3D-C[1] A30
  - 5 from SuiteSparse Matrix Collection

- COMMUNICATION ~70% - 90% FOR ALL LARGE SPARSE MATRIX SOLVES

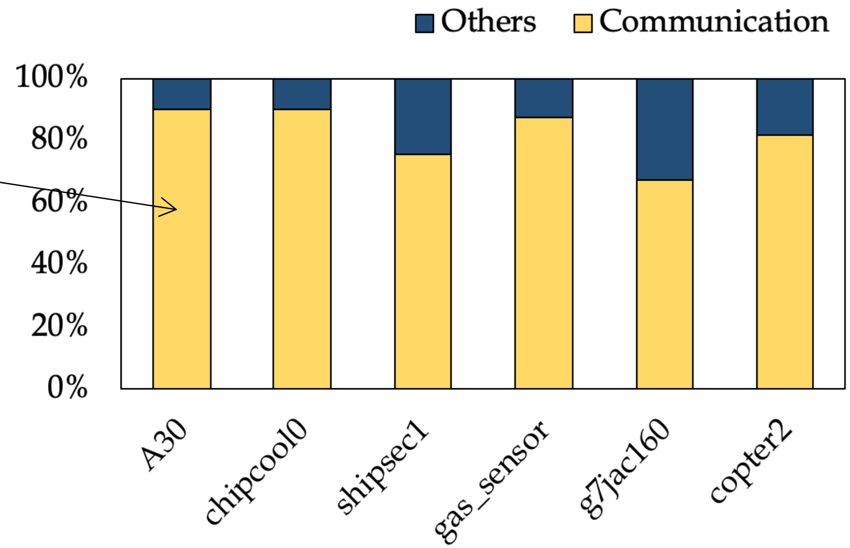

Solve time break down
on NERSC's Cori/KNL using 1024 processes

SpTRSV: SuperLU_dist triangular solve

Implementing One-Sided Communication:

- Remote direct memory access (RDMA) is a process to directly access memory on remote processes without involvement of the activities at the remote side.
- Light-weight asynchronous primitives provides a pathway to efficient DAG execution and accelerator-based exascale solvers
- Shown below: fompi one-sided communication greatly improves bandwidth over MPI two-sided

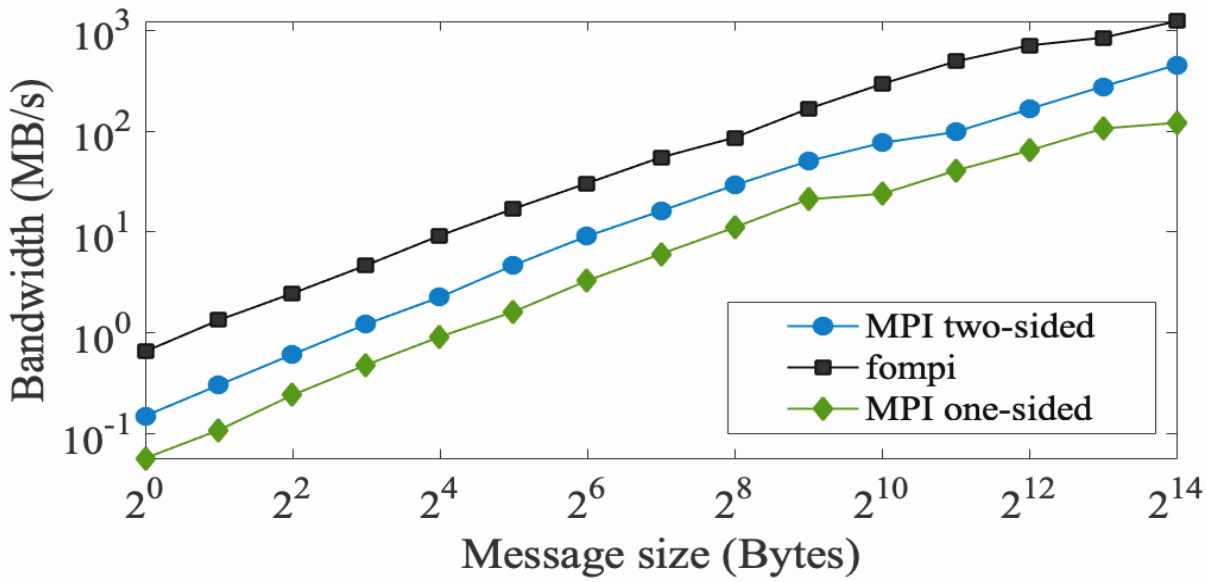

DAG: Directed Acyclic Graph

N. Ding, S. Williams, S. Li, Y. Liu

Performance model for Sparse Triangular Solvers

Critical path visualization

- LBL built a critical path analysis tool to determine the critical path with consideration of process decomposition
  - Circles can represent:
    - a DGEMV or TRSMV in SpTRSV
    - a kernel in the application
  - Edges can represent:
    - data dependencies
    - execution flow

- LBL modeled mat-vecs and communication in SpTRSV using the critical path analysis tool
  - Empirical observations of performance fit within the model's performance bounds

Critical path visualization

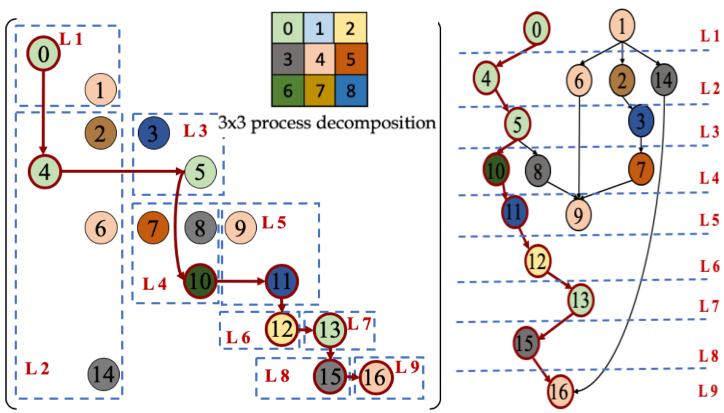

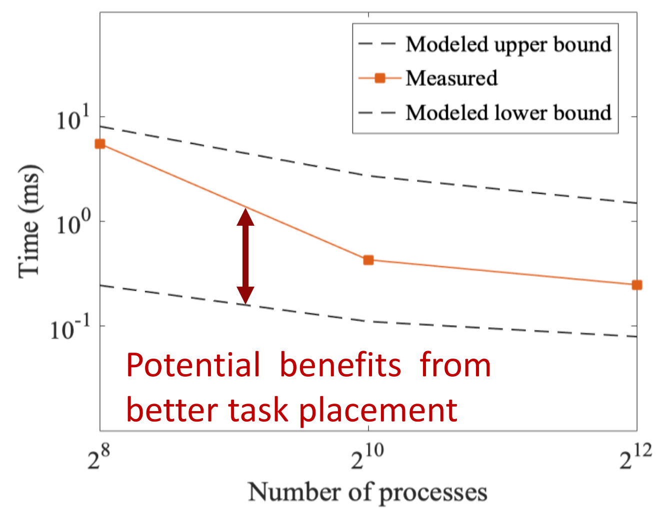

DGEMV & TRSMV are matrix-vec operations
SpTRSV: SuperLU_dist triangular solve

N. Ding, S. Williams, S. Li, Y. Liu

One-Sided Communication implemented for Sparse Triangular Solvers

- LBL created a one-sided MPI version of SpTRSV on Cray system
- Attained a 2.2x speedup for M3D-C^1 matrix at 4096 processes on Cori(NERSC) over the existing two-sided in SuperLU_DIST

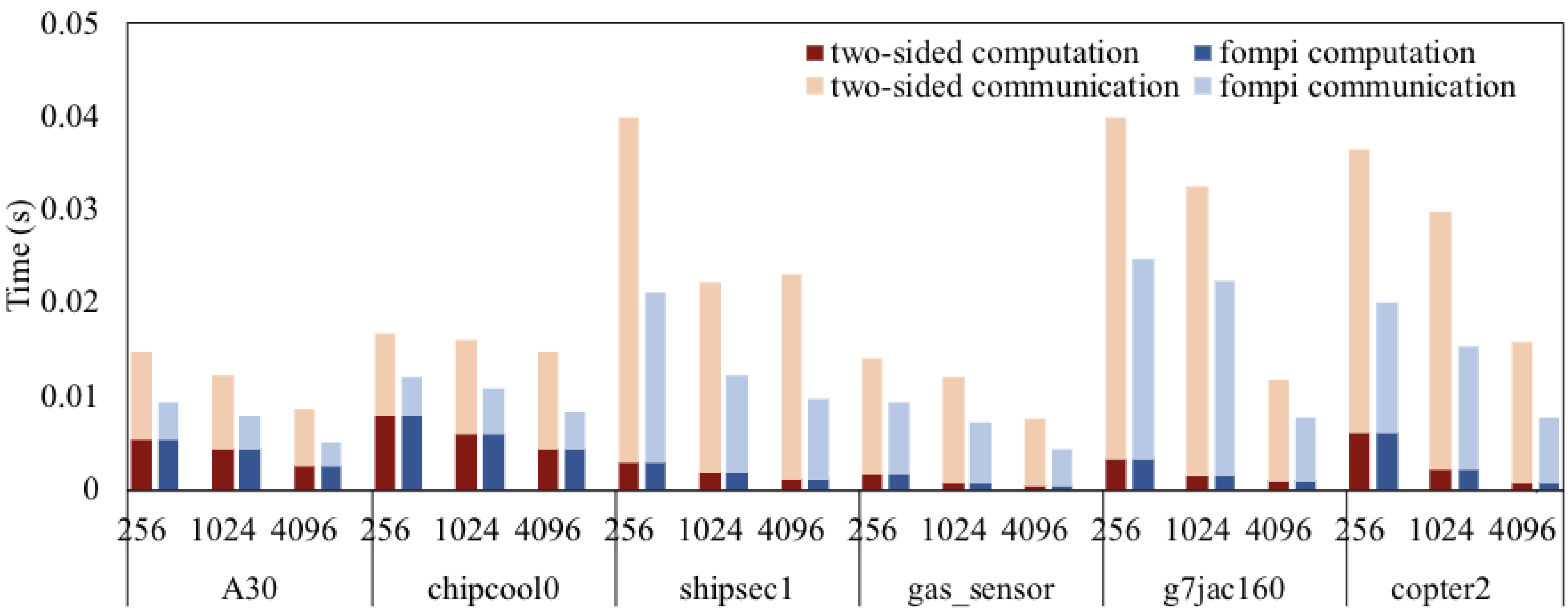

SpTRSV: SuperLU_dist triangular solve

N. Ding, S. Williams, S. Li, Y. Liu

Communication-avoiding 3D sparse LU factorization in SuperLU_dist

- **Algorithm innovation**: 3D grid of MPI processes, Z-dimension has some data replication, but results in reduced communication and increased parallelism

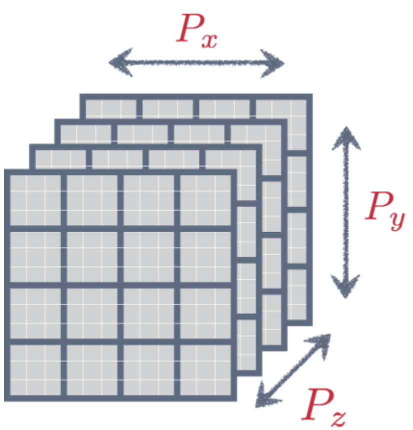

- Shown in graph is improvement in M3D-C[1] velocity matrix for 32, 128, 512 MPI processes: (1.3x, 1.8x, 5x)

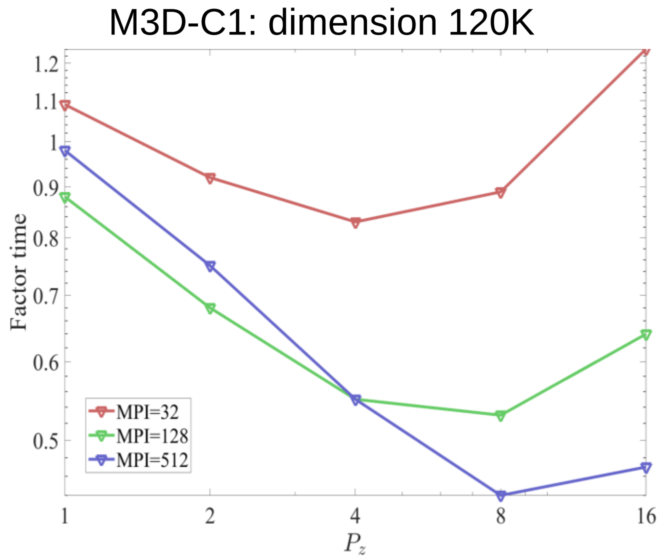

P. Sao, S. Li, Y. Liu, R. Vuduc

$\mathbf{V} = R^2 \nabla U \times \nabla \varphi + \omega R^2 \nabla \varphi + R^{-2} \nabla_\perp \chi$

Velocity Matrix Restructuring for Improved Preconditioning

- M3D-C¹ uses a physics-based Helmholtz-like decomposition of the velocity field:

$$\mathbf{V} = R^2 \nabla {\color{red}U} \times \nabla \varphi + {\color{red}\omega} R^2 \nabla \varphi + R^{-2} \nabla_\perp {\color{red}\chi}$$

- The old ordering mixed these 3, physically different velocity variables in the same vector

- New ordering allows us to separate these, facilitating a more efficient pre-conditioning strategy.

Because each toroidal plane couples only to adjacent toroidal planes, the full velocity matrix is of block-tridiagonal form. Corner elements due to periodicity.

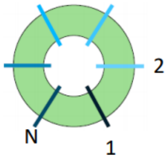

$$\begin{bmatrix} \mathbf{B}_1 & \mathbf{C}_1 & & \mathbf{A}_1 \\ \mathbf{A}_2 & \mathbf{B}_2 & \mathbf{C}_2 & \\ & \ddots & \ddots & \ddots \\ \mathbf{C}_N & & \mathbf{A}_N & \mathbf{B}_N \end{bmatrix} \bullet \begin{bmatrix} \mathbf{X}_1 \\ \mathbf{X}_2 \\ \vdots \\ \mathbf{X}_N \end{bmatrix} = \begin{bmatrix} \mathbf{Y}_1 \\ \mathbf{Y}_2 \\ \vdots \\ \mathbf{Y}_N \end{bmatrix}$$

$\mathbf{X}_j$ contains all the velocity variables on plane j

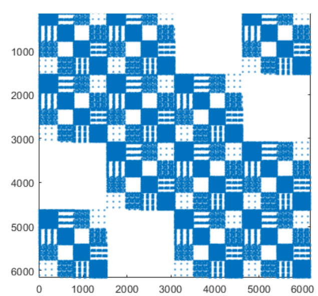

per-process

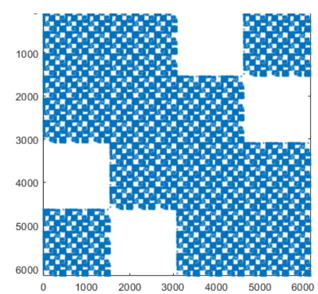

per-plane

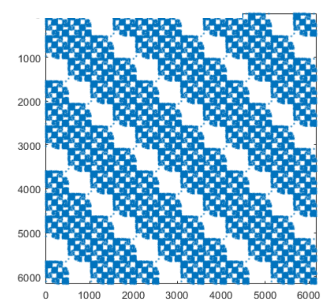

global

(R, φ, Z) coordinates

W. Tobin, M. Shephard, E. Seol

Adjacency – based reordering has potential to improve performance

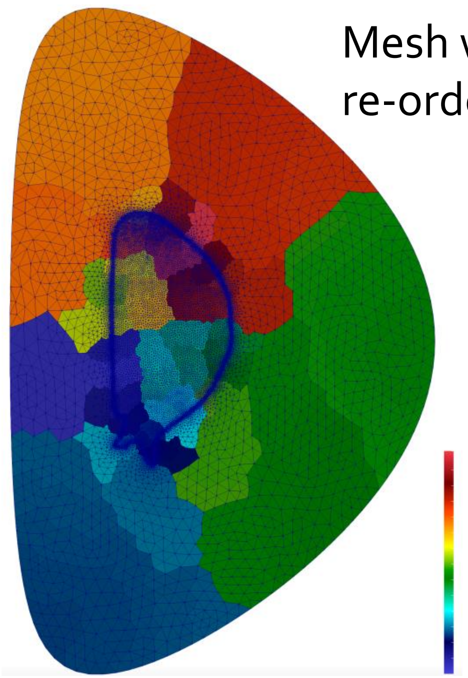

Mesh without re-ordering

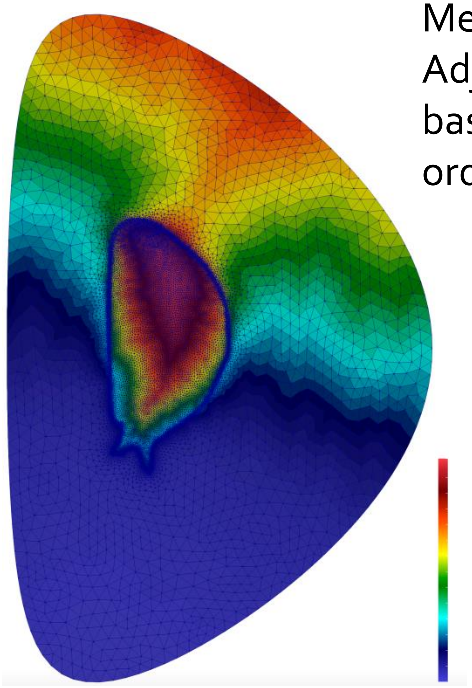

Mesh with Adjacency-based re-ordering

- Colors correspond to mesh numbering: blue → red
- Re-ordering can improve cache misses and Particle-in-Cell performance
- Now being evaluated for M3D-C^1 and NIMROD

E. Seol, M. Shephard, W. Tobin

Center for Tokamak Transient Simulations: **THANK YOU**

1. Code Descriptions

2. Forces due to Vertical Displacement Events

3. Disruption Mitigation via Impurity Injections
   3.1 Stand Alone
   3.2 via code coupling

4. Runaway Electrons interacting with MHD

5. High-Performance Computing

Extra slides